

STRUCTURAL PROPERTIES OF COMPOSITE ELASTOMERIC MEMBRANES USING SMALL-ANGLE NEUTRON SCATTERING*

E. M. ANITAS^{1,2,a}, I. BICA³, R. V. ERHAN^{1,2}, M. BUNOIU³, A. I. KUKLIN^{1,4}

¹Joint Institute for Nuclear Research, Dubna 141980, Moscow region, Russian Federation
E-mail: anitas@theor.jinr.ru ^a*Corresponding author*

²Horia Hulubei National Institute of Physics and Nuclear Engineering, RO-077125
Bucharest-Magurele, Romania

³West University of Timisoara, Timisoara, Romania

⁴Laboratory for Advanced Studies of Membrane Proteins, Moscow Institute of Physics and
Technology, Dolgoprudniy, Russian Federation

Received January 10, 2015

The morphology of elastomeric membranes based on silicone rubber, at various concentrations of the catalyst (C) is determined by small-angle neutron scattering (SANS) technique. Nearly all membranes display a hierarchical organization of crystallites in which ramified mesoscale mass fractals are composed of either mass or surface-like nano fractals. We use the Beaucage model in order to extract information about the radius of gyration of the clusters and about their fractal dimensions. We show that the fractal dimension of the mesoscale fractal is fixed at 2.68 and is independent with the addition of C . However, the nanoscale fractals are characterized by a transition from mass to surface-like fractals at high values of C concentrations.

Key words: SANS, fractals, elastomeric membranes.

1. INTRODUCTION

Recently, many scientific efforts have been directed on the optimization of structural performances of elastomeric membranes (advanced materials consisting of microparticles dispersed in an elastic matrix) as well as for determination of correlations between their structural and physical properties [1, 2]. A concise description of their structure is usually obtained using small-angle scattering (SAS) [3], which yields the differential elastic cross section as a function of momentum transfer and which describes the spatial density-density correlations of the system.

The main advantage of SAS is that it's a non-destructive method and that basic quantities of interest, averaged over a macroscopic volume, can be extracted with almost no approximation or model. Therefore, together with electron microscopy technique, they are the primarily tools for description of the microstructure of a large class of elastomeric materials, such as those with Stomaflex Creme as a matrix and filled

*Paper presented at the conference "Advanced many-body and statistical methods in mesoscopic systems II", September 1-5, 2014, Brasov, Romania.

with a ferrofluid [2, 4]. Here, the morphology of composites elastomeric membranes based on silicone rubber, filled with catalyst at various concentrations is determined by SANS. We use the Beaucage model [5], since it can describe complex hierarchical fractal structures [6, 8]. Results showing the characteristic sizes and modifications of scattering intensity with catalyst concentration are presented and analyzed.

2. THEORETICAL BACKGROUND

An important indicator of the structural type is the simple power-law decay which is characteristic to random fractals and allows us to differentiate between mass and surface fractals [7, 8]. The difference arise in the value of scattering exponent of the power-law decay in the fractal region, where $I(q) \propto q^{-\tau}$, with $\tau = D_m$ for mass and $\tau = 6 - D_s$ for surface fractals. Here D_m and D_s are the mass and, respectively, surface fractal dimension and lie within $0 < D_m < 3$ for a mass fractal, and within $2 < D_s < 3$ for surface fractals.

The same meaning of the scattering exponent holds for monodisperse deterministic fractals which gives *generalized* power-law decays (superposition of maxima and minima on a simple power-law decay) and which allows us to extract additional information from experimental SAS data [9, 10]. Therefore, the simple power-law behavior observed can be described by a system of polydisperse deterministic fractals where minima and maxima are smeared out with increasing the relative variance [8–10]. Since for these membranes it's not yet fully understood if they possess exact self-similar organization, we use Beaucage model which can give information about the shape and size of each structural level [5, 11]. The shape is obtained through the value of the scattering exponent and the size is obtained through the value of the radius of gyration. Therefore, for a two-level structure

$$I(q) \approx G_1 e^{-\frac{q^2 R_{g1}^2}{3}} + B_1 e^{-\frac{q^2 R_{g2}^2}{3}} \left(\frac{h_1}{q}\right)^{D_1} + G_2 e^{-\frac{q^2 R_{g2}^2}{3}} + B_2 \left(\frac{h_2}{q}\right)^{D_2} + B, \quad (1)$$

where $h_1 = \text{erf}(qR_{g1}/\sqrt{6})^3/q$, $h_2 = \text{erf}(qR_{g2}/\sqrt{6})^3/q$ and B is the background. The first term describes a large-scale structure of size R_{g1} composed of small-scale structures of size R_{g2} , written in the third term. The second term allows for mass- or surface fractal power-law regimes for the large structure. G_1 and G_2 are classic Guinier prefactors, and B_1 and B_2 are prefactors specific to the type of power-law scattering, specified in the regime in which the exponents D_1 and D_2 fall.

3. FABRICATION AND METHODS

Materials used in this study for fabrication of composite elastomeric membranes are: Silicone rubber (*SR*; $[\text{CH}_3]_2\text{SiCl}_2$), type RTV-3325 from Bluestar Sil-

icones; Catalyst (C ; $C_{36}H_{52}ClMnN_2O_2$), type 60R, from Rhone-Poulenc; Silicone oil (SO ; $C_6H_{18}OSi_2$), from Merck with viscosity 250 mPas at $T = 297K$ and Stearic acid (SA ; $C_{18}H_{36}O_2$), from Merck.

To obtain the membranes we prepare a mixture with a volume of $5 * 10^{-6} m^3$ which contains two components: 96 % *vol.* SO and 4 % *vol.* C . The as-obtained mixture is heated up to 350 K, and after about 300 s the mixture becomes homogeneous (SAS). Above 300 K SAS is in a liquid phase, while at temperatures below 300K, SAS is in a crystalline phase. Then, we pour a volume of $5 * 10^{-6} m^3$ SR into four Berzelius glasses. Each glass is heated up to 450 K and we add a volume of $1 * 10^{-6} m^3$ SAS (at about 330 K). The mixture from each glass is homogenized for 600 s. When the temperature of the obtained product consisting of SR and SAS is below 300 K we introduce C in various volumes. The four solutions are again homogenized, now for 300 s, after which we obtain the samples: S_1 with $0.3 * 10^{-6} m^3$, S_2 with $0.6 * 10^{-6} m^3$, S_3 with $0.9 * 10^{-6} m^3$, and S_4 with $1.2 * 10^{-6} m^3$ of C . Each obtained solution is poured between two polyethylene foils and are pressed between two plane parallel plates. After polymerization (24 h) we obtain the elastomeric membranes S_i , $i = 1, 2, 3, 4$.

SANS experiments were performed at YUMO small-angle diffractometer at the IBR-2 pulsed reactor, JINR, Dubna, Russia. A two-detector system was used and the scattering intensity, isotropic over the radial angle, on the detector was obtained as a function of the module of momentum transfer, $q = (4\pi/\lambda)\sin(\theta/2)$, where λ is the incident wavelength and θ is the scattering angle. Processing of the measured spectrum and data correction were realized using SAS [12] software.

4. RESULTS AND DISCUSSIONS

Fig. (1a) shows SANS data on a double logarithmic scale, from composite elastomeric membranes at various volume fractions of the catalyst.

For volume fraction $\phi = 5$ % of the catalyst the scattering curve (lowest curve) is characterized by two regions: at low- and intermediate- q ($q > 7.2 * 10^{-3} \text{ \AA}^{-1}$) we have a power-law decay, and at high- q ($q > 0.2 \text{ \AA}^{-1}$) the background is attained. The absolute value of the scattering exponent of this *single* power-law decay is $D = 2.68$ and since its value is smaller than 3 it coincides with the mass fractal dimension of the polymer matrix. Therefore the catalyst at $\phi = 5$ % does not have a significant effect on the highly branched structure of the membrane.

For higher volume fractions of the catalyst ($\phi = 10$ %, $\phi = 15$ % and $\phi = 20$ %) the structure of the membrane changes significantly. First, at low- q (near $7.2 * 10^{-3} \text{ \AA}^{-1}$) we can see the appearance of a Guinier region while in the intermediate region ($7.2 * 10^{-3} \text{ \AA}^{-1} < q < 0.2 \text{ \AA}^{-1}$) we have a *succession* of two power-law decays separated by a knee near $7 * 10^{-2} \text{ \AA}^{-1}$. The knee position remains the same

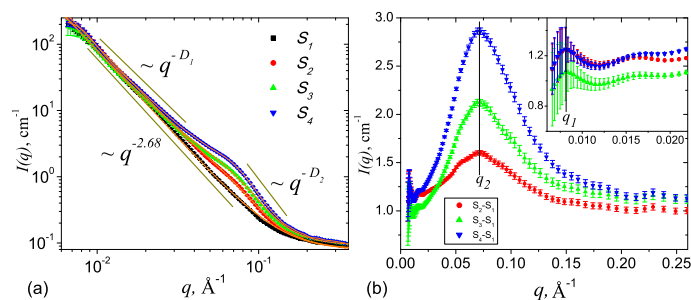


Fig. 1 – (Color online) (a) SANS intensity from membranes for various volume fractions (ϕ) of the catalyst C : a) $\phi = 5\%$ (Sample S_1); b) $\phi = 10\%$ (Sample S_2); c) $\phi = 15\%$ (Sample S_3); d) $\phi = 20\%$ (Sample S_4). S_1 is fitted with a simple power-law; S_2, S_3 and S_4 are fitted with the Beaucage model (Eq. 1). Discrete points: experimental data; Continuous lines: theoretical models. (b) SANS intensity curves from the catalyst C , obtained by subtracting the contribution of the sample S_1 from: a) S_2 ; b) S_3 ; c) S_4 . Vertical lines indicate an approximate position of the maxima at low- and high- q .

with increasing catalyst concentration, although it becomes more pronounced. Such a behavior of the scattering curve is usually associated with a two-level structure. Due to absence of a generalized power-law decay, we can't explain the system in the framework of monodisperse deterministic fractals [9, 10] and therefore Beaucage model (Eq. 1) is used to determine the features of these two-level structures. The main parameters are, for S_1 : $D = 2.68$; for S_2 : $D_1 = 2.68$, $R_{g1} = 378 \text{ \AA}$, $D_2 = 3.01$ and $R_{g2} = 28.63 \text{ \AA}$; for S_3 : $D_1 = 2.70$, $R_{g1} = 354 \text{ \AA}$, $D_2 = 3.26$ and $R_{g2} = 28.25 \text{ \AA}$; for S_4 : $D_1 = 2.69$, $R_{g1} = 381 \text{ \AA}$, $D_2 = 3.5$ and $R_{g2} = 27.65 \text{ \AA}$.

One can see the formation of a large mass fractal structure with fractal dimension nearly constant with catalyst, at about $D_1 = 2.69$ and slight variations of their radii of gyration R_{g1} . The same results show that the mass fractal is composed of surface fractal-like structures [13] whose fractal dimensions decrease (or equivalently, the exponent D_2 decreases) up to $6 - D_2 = 2.5$ while the radii of gyration are kept nearly constant at about $R_{g2} = 28 \text{ \AA}$. The decrease of fractal dimension shows that the roughness of surface fractal becomes less pronounced with increasing the catalyst.

The individual contribution of catalyst to the total scattering intensity can be obtained if we subtract from the latter one, the contribution of the elastomeric matrix. Fig. (1b) shows the scattering intensity obtained after the subtraction of elastomeric matrix contribution from each sample S_2, S_3 and S_4 . Experimental data show the formation of peaks at around $q_{c1} = 0.0084 \text{ \AA}^{-1}$ and $q_{c2} = 0.081 \text{ \AA}^{-1}$ whose positions are nearly independent of the volume fraction of the catalyst. Using the relation $d_i = 2\pi/q_i$, with $i = 1, 2$ and where d is a characteristic of the structure (domain) size, we obtain $d_1 = 748 \text{ \AA} \approx 2R_{g1}$, and respectively $d_2 = 78 \text{ \AA} \approx 2R_{g2}$. Due to the presence of well defined simple power-law decay (as opposed to slightly oscillating ones) the values of radii of gyration represent mean values over fractals with relatively large

degree of polydispersity [10], and this could explain the small discrepancies observed in their values from Beaucage model (Fig. 1a) and from peak's position (Fig. 1b).

5. CONCLUSIONS

Using SANS techniques we investigated the morphology of elastomeric membranes based on silicone rubber filled with various volume fractions ϕ of catalyst.

For $\phi = 5\%$ the catalyst does not have a significant influence on the membrane microstructure, and the latter one is characterized by a highly branched mass fractal structure with fractal dimension about $D = 2.68$. By increasing the volume fraction of the catalyst up to $\phi = 10\%$, 15% and 20% , a two-level structure consisting of crystallites is formed: first, a mesoscale mass fractal structure with an average radius of gyration $R_{g1} \approx 368 \text{ \AA}$ and a nearly constant fractal dimension $D = 2.68$ (the same as for $\phi = 5\%$) indicating that in this q -range the effect of catalyst is insignificant regarding the degree of polymer branching; second, a nanoscale mass and surface fractal-like structure with a nearly constant value of the radius of gyration $R_{g2} \approx 37.7 \text{ \AA}$ and with a decreasing value of the fractal dimension. At this scale the morphology of the membrane is significantly changed and a transition occurs from a mass fractal ($\phi = 10\%$) to a rough surface fractal-like structure ($\phi = 20\%$).

Acknowledgements. Support from JINR IFIN - HH grants is acknowledged. A.I. Kuklin acknowledges support by program '5Top100' of Ministry of Education and Science of Russian Federation.

REFERENCES

1. M. Balasoiu, E. M. Anitas, I. Bica, R. Erhan, V. A. Osipov, O. L. Orelovich, D. Savu, S. Savu, A. I. Kuklin, *Optoelectronics and Advanced Materials - Rapid Communications*, **2**(11), 730 (2008).
2. E. M. Anitas, M. Balasoiu, I. Bica, V. A. Osipov, A. I. Kuklin, *Optoelectronics and Advanced Materials - Rapid Communications*, **3**(6), 621 (2009).
3. O. Glatter, O. Kratky, *Small-angle X-ray Scattering* (London, & Academic Press, 1982).
4. M. Balasoiu, M. L. Craus, E. M. Anitas, I. Bica, J. Plestil, A. I. Kuklin, *Phys. Sol. State*, **52**(5), 917 (2010).
5. G. Beaucage, *J. Appl. Cryst.*, **28**, 717–728 (1995).
6. E. M. Anitas, *Eur. Phys. J. B*, **87**, 139 (2014).
33, 269 (1986).
7. J. E. Martin, *J. Appl. Cryst.*, **87**, 20 (1987).
8. P. W. Schmidt, *J. Appl. Cryst.*, **24**, 414–435 (1991).
9. A. Yu. Cherny, E. M. Anitas, A. I. Kuklin, M. Balasoiu, V. A. Osipov, *J. Appl. Cryst.* **43**, 790 (2010).
10. A. Yu. Cherny, E. M. Anitas, V. A. Osipov, A. I. Kuklin, *Phys Rev. E* **84**, 036203 (2011).
11. G. Beaucage, D. W. Schaefer, *J. Non-Crystalline Solids*, **172**, 797–805 (1994).
12. A. G. Soloviev *et al.*, JINR preprint **P10**-2003-86.
13. A. Yu. Cherny, E. M. Anitas, V. A. Osipov, A. I. Kuklin, *J. Appl. Cryst.* **47**, 198–206 (2014).